ispiacademy : Pages:1–22

Original Research

Risk Assessment Framework for Gas Kick Events in Complex Drilling Environments: Methods, Metrics, and Mitigation Measures

Suman Thapa[1] and Kiran Shahi[2]

[1] Tribhuvan University, Kirtipur Road, Kirtipur 44618, Kathmandu, Nepal.
[2] Pokhara University, Dhungepatan Road, Pokhara 33700, Nepal.

Abstract

Gas kick events remain a recurring operational challenge in drilling, especially in complex trajectories where pressure windows are narrow and operational variability is significant. Modern wells with extended reach, high-pressure high-temperature conditions, and managed-pressure drilling introduce coupled physical and decision-making complexities that motivate an integrated risk view. This paper develops a structured framework for risk assessment of gas kick events that combines mechanistic modeling of wellbore hydraulics, probabilistic metrics, and data-driven detection. The framework covers gas influx initiation, transient multiphase flow in the wellbore, and surface detection signals under realistic monitoring constraints. Deterministic models provide pressure and flow predictions that are interpreted within a probabilistic setting to quantify likelihoods of operational exceedances such as loss of primary well control or approach to fracture limits. Statistical and machine-learning components are used to integrate heterogeneous sensor streams and to derive early warning indicators calibrated to site-specific noise and operational patterns. The proposed structure supports quantitative risk indices that can be updated in real time as measurements are acquired and operational conditions evolve. Emphasis is placed on explicit representation of uncertainty, including variability in formation pressures, friction factors, equipment response, and human decision processes. The paper discusses numerical implementation aspects, including stability constraints for transient simulators and their interaction with real-time inference and decision support. The overall framework is intended to be adaptable across different drilling environments and operational philosophies, and to provide a consistent basis for evaluating mitigation measures such as kick tolerance design, managed-pressure strategies, and automated shut-in logic.

1. Introduction

Gas kicks arise when the bottom-hole pressure falls below the local pore pressure and formation fluids enter the wellbore, potentially evolving into loss of primary well control if not handled in a timely way [1]. In conventional vertical wells, pressure management and kick response procedures are standardized, while in complex wells the interaction of well geometry, heterogeneous formations, and active pressure-management equipment leads to a wider range of possible influx scenarios. Complex drilling environments include three-dimensional trajectories with long horizontal sections, high-pressure high-temperature reservoirs, depleted zones, tight pressure windows, and managed-pressure drilling systems with dynamic choke and back-pressure control [2]. In such settings, gas kicks may develop in more subtle ways, with smaller initial inflow rates, non-intuitive transient responses, and detection signals that are more difficult to distinguish from routine operational changes.

Traditional risk assessments for gas kicks often decompose the problem into static barrier diagrams and deterministic engineering calculations of kick tolerance and shut-in responses. While such approaches remain widely used, they may under-represent uncertainties in formation properties, equipment behavior, and human response time, particularly when the drilling program evolves during

Table 1: Core components of the gas kick risk assessment framework

Component	Domain	Primary role	Representative outputs
Deterministic hydraulics	Wellbore / surface	Simulate multiphase flow, pressures, and influx dynamics along the wellbore	Bottom-hole pressure trajectory, gas volume fraction profiles, surface flow-out and choke response
Probabilistic risk module	Uncertainty / statistics	Propagate uncertain inputs to event probabilities and risk indices	$P_{\text{kick}}(t)$, $P_{\text{frac}}(t)$, $R(T)$, exceedance probabilities
Machine-learning detection	Data-driven signals	Map multi-sensor time series to kick likelihood and early warning indicators	$\hat{P}_{\text{ML}}(t)$, anomaly scores, classification labels
Decision and control logic	Operations	Translate risk indicators into recommended actions under operational constraints	Alert levels, recommended pump/choke adjustments, shut-in recommendations
Uncertainty representation	Cross-cutting	Maintain and update distributions for key parameters and model errors	Posterior samples of X, ensemble statistics, sensitivity indicators

operations [3]. Furthermore, increasing volumes of real-time measurements from surface and downhole sensors provide opportunities to move from static calculations toward dynamically updated risk estimates. A systematic framework that combines mechanistic models, probabilistic metrics, and data-driven analytics can support more consistent decision-making under uncertainty and facilitate evaluation of alternative mitigation strategies.

This paper develops such a framework for gas kick risk assessment in complex drilling environments. The focus is on integrating three principal components. The first component is a deterministic, physics-based representation of gas influx and transient wellbore hydraulics that is suitable for real-time or near real-time simulation. The second component is a probabilistic description of uncertainties and risk metrics that translate model outputs and measurements into interpretable quantities such as likelihood of loss of primary well control or proximity to fracture limits [4]. The third component is a data-driven detection and early warning layer that interprets multi-sensor data streams and provides inputs to the probabilistic risk module. The framework is structured to accommodate different drilling philosophies, including conventional and managed-pressure drilling, and to support both planning-phase analysis and operational decision support.

The paper is organized around a sequence of modeling and inference steps [5]. Gas kick mechanisms and the characteristics of complex drilling environments are first described in terms of pressure balance, influx pathways, and monitoring signals. A deterministic transient model of multiphase flow in the wellbore is then formulated, based on one-dimensional conservation equations and closure relations for gas-liquid flow, with discussion of numerical solution strategies. Probabilistic risk metrics are introduced, together with estimation procedures for model-parameter uncertainties and validation of

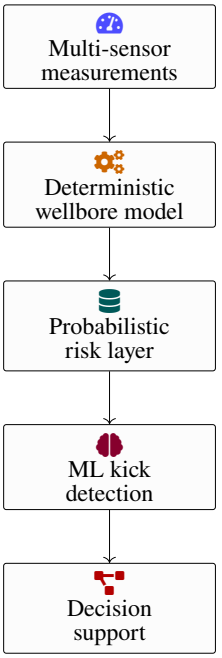

Figure 1: Integrated architecture for gas kick risk assessment. Measurements from surface and downhole sensors feed a deterministic wellbore model, which is embedded in a probabilistic layer to compute risk measures such as P_{kick} and P_{frac}. A machine-learning component provides data-driven kick indicators that, together with model-based risk metrics, support operational decision-making.

exceedance probabilities [6] [7]. A machine-learning-based detection layer is described that fuses surface and downhole measurements into probabilistic kick indicators. These elements are finally combined into an integrated risk assessment and mitigation framework that structures the flow of information from sensors and models to risk metrics and operational decisions.

2. Gas kick mechanisms and complex drilling environments

Gas kicks are initiated when the bottom-hole pressure, including hydrostatic and frictional components, falls below the formation pore pressure at some location along the open hole or within a permeable interval [8]. Let z denote measured depth along the wellbore, with $z = 0$ at the surface and increasing downward, and consider a column of drilling fluid with density $\rho_f(z,t)$. The static hydrostatic pressure profile in the absence of flow is given by

$$p_{\text{hyd}}(z) = p_s + \int_0^z \rho_f(\xi) g \, d\xi, \tag{2.1}$$

where p_s is surface pressure, g is gravitational acceleration, and ξ is an integration variable [9]. During drilling, circulation and pipe movement modify this profile through frictional losses and dynamic effects. Denoting the frictional pressure loss per unit length by $\lambda_f(z,t)$, the approximate circulating bottom-hole pressure can be written as [10]

$$p_{\text{bh}}(t) \approx p_s(t) + \int_0^{z_{\text{bh}}} \rho_f(\xi,t) g \, d\xi - \int_0^{z_{\text{bh}}} \lambda_f(\xi,t) \, d\xi, \tag{2.2}$$

where z_{bh} is the depth of the bit or open-hole end. A gas kick may occur when $p_{\text{bh}}(t)$ falls below the local pore pressure $p_p(z)$ at a permeable interval, either due to a reduction in mud density, a transient

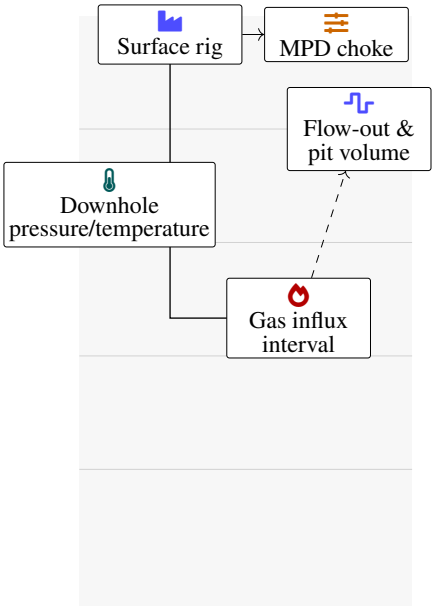

Figure 2: Schematic of a complex well with an extended horizontal section, highlighting a gas influx interval, managed-pressure choke, and key monitoring points. The well trajectory traverses heterogeneous formations, while sensors at surface and downhole locations provide pressure, temperature, and flow signals. A localized influx in the horizontal section may lead to subtle and delayed responses at surface sensors, motivating combined use of mechanistic models and data-driven detection.

swab effect during pipe movement, an abrupt change in flow regime, or an unplanned loss of surface back-pressure.

In complex drilling environments, several features modify the onset and evolution of kicks compared to simpler wells. Extended-reach trajectories often include long horizontal sections, in which gravitational segregation of gas and liquid phases is more pronounced and frictional pressure losses may differ from those predicted by vertical correlations. High-pressure high-temperature reservoirs may exhibit strong temperature gradients and non-linear fluid properties, with density and viscosity dependent on both pressure and temperature [11]. Depleted zones adjacent to high-pressure intervals create narrow pressure windows, where the difference between pore pressure and fracture pressure is small, and where small changes in mud density or flow regime can shift the system toward kick or losses.

Managed-pressure drilling (MPD) adds further complexity by introducing active surface equipment that manipulates annular back-pressure and flow paths. In MPD, the effective bottom-hole pressure is a combination of hydrostatic, frictional, and controlled back-pressure components [12]. The system reacts to changes in flow or pressure through control loops that adjust choke positions and pump rates, leading to coupled dynamics between reservoir inflow, wellbore hydraulics, and control logic. From a risk perspective, MPD may reduce the frequency of kicks for a given mud weight but can also change the character of detection signals, since flow and pressure deviations may be partially compensated by the control system before they become apparent in raw measurements.

The presence of complex geometry and heterogeneous formations also affects monitoring [13]. Surface flow-out, pump strokes, standpipe pressure, and pit volume are standard signals used for kick detection. In complex wells, additional signals such as downhole pressure and temperature, distributed fiber-optic measurements, and choke pressures are often available. These sensors have different latencies, noise properties, and spatial sensitivities [14]. For example, a small influx at a deep horizontal section may take a considerable time to affect surface flow-out, while it may appear earlier in downhole pressure or fiber-optic temperature if these sensors are present. The spatial distribution of gas along the wellbore, driven by slip and segregation, will influence the amplitude and timing of these signals.

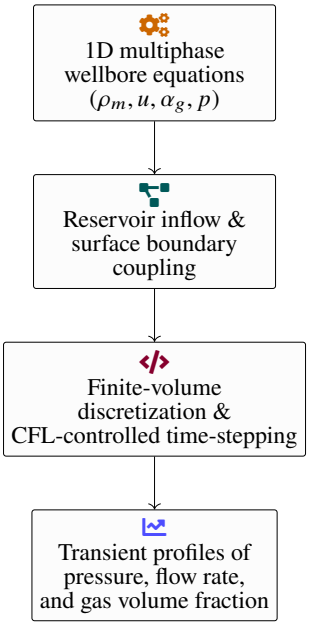

Figure 3: Structure of the deterministic wellbore model used for gas kick simulation. Mixture conservation equations with drift-flux closure are coupled to reservoir inflow relations and surface pump/choke conditions. A finite-volume scheme with appropriate CFL constraints advances the model in time, delivering transient predictions of pressure, flow, and gas distribution along the wellbore.

Complex operational sequences, such as connections, tripping, reaming, and managed-pressure transitions, further complicate interpretation of signals, because they induce transient changes in flow and pressure that can resemble kick signatures [15]. A connection event, for instance, normally involves pump stoppage and restart, leading to transient reductions and increases in standpipe pressure and flow-out. Distinguishing such routine operational transients from small influx signals requires both mechanistic understanding and data-driven pattern recognition. The risk assessment framework considered in this paper therefore treats kicks as events embedded in a background of operational variability, recognizing that detection thresholds and false-alarm rates depend on this context [16].

3. Deterministic modeling of gas influx and wellbore transients

A deterministic model of gas kicks in complex wells aims to represent the coupled dynamics of multiphase flow in the wellbore, reservoir inflow, and surface equipment. For risk assessment, the model needs to capture the main features that influence pressure evolution, influx volume, and key detection signals, while being computationally tractable. A common starting point is a one-dimensional representation of the annulus and drillstring, with depth coordinate z and time t [17]. The flow in the annulus is usually modeled using mixture conservation equations for mass and momentum, with gas and liquid phases represented through a slip or drift-flux formulation.

Let $\alpha_g(z,t)$ denote the gas volume fraction, ρ_l the liquid density, and $\rho_g(z,t)$ the gas density [18]. The mixture density is

$$\rho_m = \alpha_g \rho_g + (1 - \alpha_g)\rho_l. \tag{3.1}$$

Assuming a single mixture velocity $u(z,t)$ in the annulus and cross-sectional area $A(z)$, the mass conservation equation can be written as

$$\partial_t(\rho_m A) + \partial_z(\rho_m A u) = q_m, \tag{3.2}$$

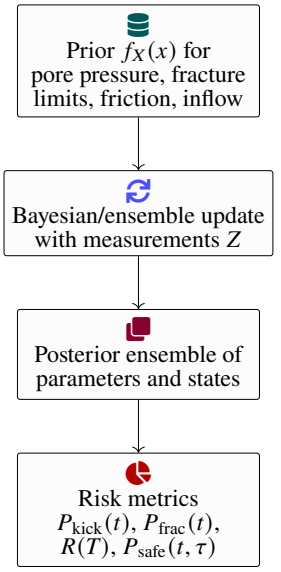

Figure 4: Probabilistic layer that maps uncertainty in model inputs and measurements to risk metrics. A prior distribution over uncertain parameters is updated with incoming data to form a posterior ensemble, which is propagated through the deterministic simulator. Event probabilities and consequence-based indices are computed from the resulting distributions of pressures, influx volumes, and trajectory-wide safety margins.

where $q_m(z,t)$ represents distributed mass sources, including gas influx from the formation [19]. The mixture momentum balance can be written in the form

$$\partial_t(\rho_m A u) + \partial_z(\rho_m A u^2) + A\,\partial_z p = \rho_m A g\cos\theta - \tau_w P_w, \tag{3.3}$$

where $p(z,t)$ is pressure, $\theta(z)$ is the local inclination angle, $\tau_w(z,t)$ is the wall shear stress, and $P_w(z)$ is the wetted perimeter. Closure relations are needed to express τ_w in terms of mixture properties and to define the gas distribution and slip between phases [20].

Gas dynamics are often represented using a drift-flux relation between gas and mixture velocities. Denoting the gas velocity by u_g, a common closure is

$$u_g = C_0 u + V_d, \tag{3.4}$$

where C_0 is the distribution parameter and V_d is a drift velocity term dependent on flow regime and fluid properties [21]. The gas volume fraction is advanced using a transport equation of the form

$$\partial_t \alpha_g + u_g\,\partial_z \alpha_g = S_g, \tag{3.5}$$

where $S_g(z,t)$ accounts for gas sources and sinks, including inflow from the formation and possible dissolution or loss. The wall shear stress is often parameterized using a friction factor f_m for the mixture, [22]

$$\tau_w = \frac{1}{2} f_m \rho_m u|u|, \tag{3.6}$$

where f_m depends on Reynolds number and relative roughness, possibly modified for multiphase effects.

The gas density is determined by a thermodynamic relation. For simplicity, one may adopt an isothermal real-gas equation of state of the form [23]

$$\rho_g = \frac{p M_g}{ZRT}, \tag{3.7}$$

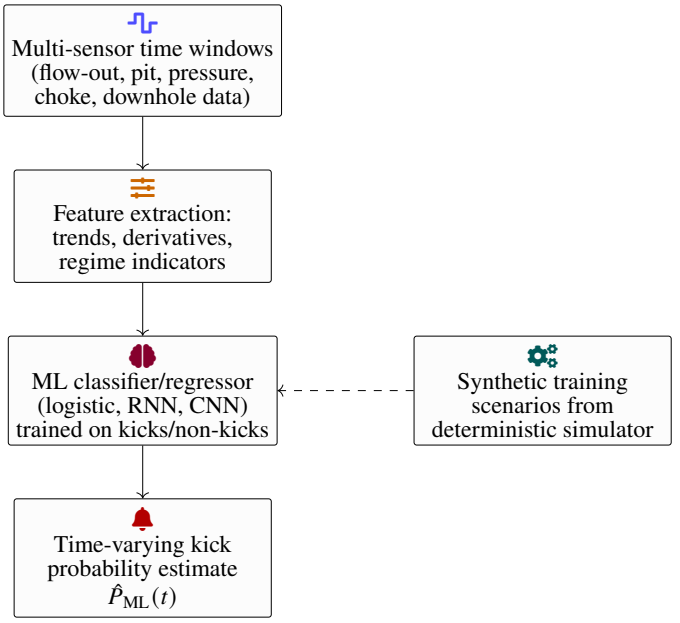

Figure 5: Machine-learning pipeline for kick detection and early warning. Sliding windows of multi-sensor signals are transformed into compact feature vectors, which are input to a supervised model trained on labeled kick and non-kick intervals. Synthetic scenarios from the wellbore simulator can augment limited historical data, and the resulting model outputs a calibrated probability of kick presence or onset as a function of time.

where M_g is the gas molar mass, $Z(p,T)$ is a compressibility factor, R is the gas constant, and $T(z,t)$ is temperature. In many operational simulations, temperature is approximated by a prescribed profile based on geothermal gradient and circulation effects, though fully coupled energy equations can be included when necessary. The liquid density ρ_l may also depend on pressure and temperature, particularly for oil-based muds, but is often treated as weakly compressible [24].

Formation inflow is represented by coupling the wellbore pressure to a reservoir model. For a given permeable interval at depth $z = z_r$, an inflow rate q_g of gas into the wellbore can be modeled as

$$q_g = J_g \left(p_p - p(z_r,t)\right), \tag{3.8}$$

where J_g is an inflow productivity index and p_p is the local pore pressure [25]. This expression reflects Darcy-type inflow under slightly compressible conditions; more detailed models may incorporate non-linearities, phase behavior, and multi-layer interactions. For risk assessment, the key aspect is the sensitivity of influx rate to bottom-hole pressure and the uncertainty in both J_g and p_p [26].

Surface boundary conditions are defined by the interaction between pumps, choke, and separator systems. At the standpipe, pump flow imposes a volumetric inflow rate, while at the annulus outlet the choke pressure and flow relation introduces a non-linear boundary. A simple representation of choke behavior is [27]

$$q_{\mathrm{ch}} = C_c A_c \sqrt{\frac{2(p_u - p_d)}{\rho_m}}, \tag{3.9}$$

where q_{ch} is choke flow rate, C_c is a discharge coefficient, A_c is choke area, and p_u, p_d are upstream and downstream pressures. Managed-pressure drilling modifies p_d through controlled back-pressure, while in conventional drilling atmospheric conditions typically fix p_d near constant. The coupling to the wellbore model produces feedback between pressure, flow, and choke setting.

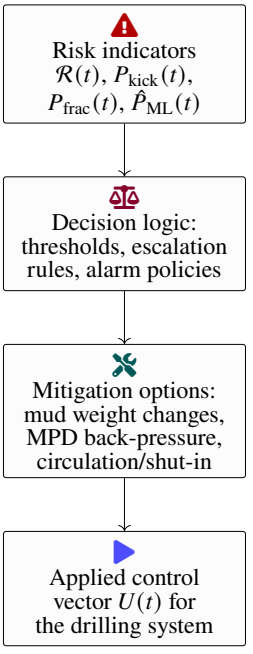

Figure 6: Decision structure linking quantitative risk indicators to operational controls. Combined probabilistic and data-driven measures are mapped to alarm states and escalation rules, which in turn select among available mitigation options such as density adjustments, managed-pressure strategies, and controlled shut-in. The chosen action is expressed as a control vector applied to pumps, choke, and related equipment, closing the loop between risk assessment and well control execution.

The system of equations is discretized in space and time for numerical solution [28]. Finite volume methods are commonly used to preserve conservation properties, with control volumes defined along the depth coordinate. Let Δz denote the spatial step and Δt the time step. A semi-discrete form of the mass balance for cell i can be written as [29]

$$\frac{d}{dt}(\rho_{m,i} A_i \Delta z) = F_{i-1/2} - F_{i+1/2} + Q_{m,i}, \tag{3.10}$$

where $F_{i\pm1/2}$ are numerical fluxes at cell interfaces and $Q_{m,i}$ is the integrated source term. Stability considerations lead to constraints on Δt based on the Courant–Friedrichs–Lewy (CFL) condition, which in simplified form can be expressed as

$$\Delta t \leq \text{CFL} \frac{\Delta z}{|u| + c_m}, \tag{3.11}$$

where c_m is a characteristic mixture wave speed and CFL is a chosen stability factor. Implicit time-stepping schemes can relax this constraint but require solution of non-linear algebraic systems at each step, which must be balanced against real-time computational requirements in operational settings.

The deterministic model described above provides time-dependent predictions of pressure, flow rate, gas volume fraction, and related variables along the wellbore [30]. For risk assessment, key outputs include bottom-hole pressure trajectories, total influx volume as a function of time, surface flow-out signals, and possible approach to fracture or equipment limits. These outputs are sensitive to uncertain inputs such as formation pore pressure, friction factors, gas properties, and operational parameters. In the next section, these uncertainties are treated probabilistically to define risk metrics [31].

Table 2: Characteristics of complex drilling environments relevant for gas kicks

Feature	Impact on kick behavior	Modeling implications	Detection challenges
Extended-reach and long horizontal sections	Enhanced gravitational segregation and gas holdup; prolonged transport times to surface	Inclination-dependent friction and slip models; careful representation of phase distribution along z	Small deep influxes may be strongly attenuated before reaching surface flow-out measurements
High-pressure high-temperature (HPHT) reservoirs	Strong sensitivity of densities and viscosities to p–T variations	Pressure- and temperature-dependent fluid properties; possible coupling to an energy equation	Changes in signal amplitude and timing as circulation conditions alter the thermal state
Narrow pressure windows	Small variations in mud weight or friction can trigger kicks or losses	Accurate pore and fracture pressure envelopes; tight bounds on $\Delta p_{\min}$ and Δp_{frac}	Elevated false-alarm risk if thresholds are set too conservatively
Depleted zones near high-pressure intervals	Highly heterogeneous inflow and loss behavior along the wellbore	Layered reservoir inflow representation and spatially variable $p_p(z)$ and J_g	Overlapping signatures from influx and losses complicate interpretation
Managed-pressure drilling (MPD) systems	Active back-pressure control modifies bottom-hole pressure dynamics	Coupled representation of choke, back-pressure pump, and control logic in boundary conditions	Control action can partially mask early kick signatures in raw surface measurements
Complex operational sequences	Routine transients can resemble kick onset in pressure and flow signals	Explicit modeling of operational steps and transient hydraulics	Requires pattern recognition to distinguish operational events from true influx

4. Probabilistic risk metrics and statistical calibration

A risk assessment framework for gas kicks requires translation of uncertain model inputs and noisy measurements into probabilities of events of interest. Let X denote a vector of uncertain parameters and inputs, including formation pore pressures, fracture gradients, friction factors, inflow indices, and operational variables such as pump characteristics and choke coefficients. Let $Y(t)$ denote a vector of model outputs at time t, including bottom-hole pressure, surface flow-out, and gas fraction distributions [32]. Uncertainty in X induces uncertainty in $Y(t)$, and risk metrics are defined as functionals of this induced distribution.

A basic risk quantity is the probability that bottom-hole pressure falls below an acceptable margin above pore pressure. Let $p_{\mathrm{bh}}(t;X)$ denote the modeled bottom-hole pressure and $p_p(z_{\mathrm{bh}};X)$ the pore pressure at the relevant depth, both dependent on uncertain inputs. Define a safety margin $\Delta p_{\min}$. The

Table 3: Selected notation for the deterministic gas influx and wellbore model

Symbol	Description	Units
z	Measured depth coordinate along the wellbore, positive downward	m
t	Time variable for transient simulations	s
$p_{\mathrm{bh}}(t)$	Bottom-hole pressure, including hydrostatic and frictional components	Pa (or MPa)
$\alpha_g(z,t)$	Gas volume fraction in the annulus mixture	–
$\rho_m(z,t)$	Mixture density, $\rho_m = \alpha_g\rho_g + (1-\alpha_g)\rho_l$	$\mathrm{kg\,m^{-3}}$
$u(z,t)$	Mixture velocity in the annulus	$\mathrm{m\,s^{-1}}$
$q_g(z_r,t)$	Gas inflow rate from the formation at permeable interval z_r	$\mathrm{kg\,s^{-1}}$ or $\mathrm{m^3\,s^{-1}}$ (standard)

Table 4: Summary of governing equations in the transient multiphase wellbore model

Equation	Representative expression	Physical role
Mixture mass balance	$\partial_t(\rho_m A) + \partial_z(\rho_m A u) = q_m$	Conserves total mass of gas and liquid in the annulus, accounting for distributed sources and sinks
Mixture momentum balance	$\partial_t(\rho_m A u) + \partial_z(\rho_m A u^2) + A\,\partial_z p = \rho_m A g\cos\theta - \tau_w P_w$	Describes acceleration of the mixture due to pressure gradients, gravity, and wall shear stress
Gas volume-fraction transport	$\partial_t \alpha_g + u_g \partial_z \alpha_g = S_g$	Tracks spatial redistribution of free gas and its interaction with formation inflow or loss
Gas equation of state	$\rho_g = \dfrac{pM_g}{ZRT}$	Relates gas density to pressure and temperature via a real-gas compressibility factor Z
Formation gas inflow	$q_g = J_g\big(p_p - p(z_r,t)\big)$	Couples wellbore pressure to reservoir pore pressure and productivity at permeable intervals
Choke flow boundary condition	$q_{\mathrm{ch}} = C_c A_c \sqrt{\dfrac{2(p_u - p_d)}{\rho_m}}$	Links upstream pressure and mixture density to outflow rate through the surface choke

event of interest can be written as [33]

$$E_{\mathrm{kick}}(t) = \left\{ p_{\mathrm{bh}}(t;X) < p_p(z_{\mathrm{bh}};X) + \Delta p_{\mathrm{min}} \right\}. \tag{4.1}$$

The time-dependent probability of entering this event is

$$P_{\mathrm{kick}}(t) = \mathbb{P}\left(E_{\mathrm{kick}}(t)\right) = \mathbb{E}\left[I_{E_{\mathrm{kick}}(t)}(X)\right], \tag{4.2}$$

Table 5: Categories of uncertain parameters in gas kick risk assessment

Category	Example parameters	Typical distribution choices	Main data sources
Pore and fracture pressures	$p_p(z)$, $p_{\mathrm{frac}}(z)$, safety margins $\Delta p_{\min}$, Δp_{frac}	Normal or truncated normal with depth-dependent mean and variance	Offset wells, geomechanical models, formation tests
Friction and rheology	Mixture friction factor f_m, rheological parameters, roughness	Lognormal or beta distributions to enforce bounds and positivity	Flow-loop tests, calibration against circulation data
Reservoir inflow properties	Productivity indices J_g, layer connectivity, relative permeabilities	Lognormal or mixture models capturing heterogeneity	Well tests, reservoir models, analog fields
Equipment and control parameters	Pump efficiency, choke discharge coefficient C_c, control-loop gains	Uniform ranges or weakly informative priors	Vendor data, factory tests, on-site tuning records
Operational and human factors	Detection and decision delays, procedural compliance, response strategies	Scenario-based discrete distributions or hierarchical priors	Incident reports, expert elicitation, training exercises

where I_E is the indicator function of event E. An analogous event $E_{\mathrm{frac}}(t)$ can be defined for exceeding fracture pressure at any depth, with corresponding probability $P_{\mathrm{frac}}(t)$. These probabilities depend on the joint distribution of uncertain inputs and on the deterministic model mapping $X \mapsto Y(t)$ [34].

To characterize kick severity, one may introduce a random variable representing influx volume $V_{\mathrm{inf}}(T; X)$ accumulated over a time horizon T. Severity thresholds can be specified, for example the probability that influx volume exceeds a given tolerance V_{tol},

$$P_{\mathrm{sev}}(T) = \mathbb{P}\left(V_{\mathrm{inf}}(T; X) > V_{\mathrm{tol}}\right). \tag{4.3}$$

The joint behavior of onset and severity can be represented through a risk measure that combines likelihood and consequence. A simple expected-loss risk index can be defined as

$$R(T) = \mathbb{E}\left[C\left(V_{\mathrm{inf}}(T; X)\right)\right], \tag{4.4}$$

where $C(\cdot)$ is a non-negative consequence function that increases with influx volume and may include step changes at operational thresholds [35].

Uncertainties in X are described by probability distributions informed by offset-well data, geomechanical models, laboratory measurements, and expert judgment. In many applications, a mixture of parametric and non-parametric representations is convenient. For example, pore pressure at a given depth might be modeled as a normal random variable with mean and variance estimated from nearby wells, while friction factors may be described by lognormal distributions to ensure positivity [36]. Correlations between parameters, such as between pore pressure and fracture gradient, can be modeled through joint distributions or copulas. Let $f_X(x)$ denote the joint probability density of X. The expected

Table 6: Comparison of machine-learning approaches for kick detection

Model type	Strengths	Limitations	Example use in this context
Logistic regression	Simple, interpretable coefficients; fast training and inference	Limited ability to capture strong nonlinear interactions unless features are engineered	Baseline classifier using aggregated features from flow-out, standpipe pressure, and pit volume
Gradient-boosted trees	Handles nonlinearities and mixed feature types; robust to moderate noise	Can be prone to overfitting and less transparent than linear models	Offline model for ranking influential features and generating feature importance profiles
Convolutional neural network (CNN) on time windows	Learns local temporal patterns and edges in multi-channel time series	Requires larger labeled datasets; architecture selection can be sensitive	Detection of subtle shape changes in pressure and flow signals around connection events
Recurrent network (GRU/LSTM)	Captures longer temporal dependencies and context in operations	Higher computational cost and tuning complexity; more difficult to interpret	Streaming estimation of $\hat{P}_{\mathrm{ML}}(t)$ based on recent multi-sensor history
Hybrid physics-informed model	Augments data-driven inputs with mechanistic features or constraints	Requires careful design of physics–ML coupling and feature engineering	Using modeled $p_{\mathrm{bh}}(t)$, predicted influx rates, and measured signals jointly as inputs
Unsupervised anomaly detector	Does not require labeled kick examples; can adapt to site-specific normal behavior	Output must be calibrated to kick probability; sensitive to concept drift	Flagging deviations from routine operational patterns as candidates for operator review

values defining risk indices are then integrals of the form [37]

$$R(T) = \int C\left(V_{\mathrm{inf}}(T;x)\right) f_X(x)\, dx, \tag{4.5}$$

which are generally evaluated approximately using sampling methods or surrogate models.

Parameter calibration and uncertainty quantification rely on statistical inference using measurements collected during drilling. Let Z denote observed data, consisting of time series of pressures, flow rates, and other signals [38]. A Bayesian formulation is natural in this context. Starting from a prior distribution $f_X^{\mathrm{prior}}(x)$ representing initial beliefs about uncertain inputs, the posterior distribution given data is

$$f_X^{\mathrm{post}}(x|Z) \propto L(Z|x) f_X^{\mathrm{prior}}(x), \tag{4.6}$$

where $L(Z|x)$ is the likelihood of observations given parameters. The likelihood is determined by the deterministic model, measurement functions, and noise assumptions [39]. If η denotes measurement

Table 7: Layers of the integrated risk assessment and decision framework

Layer	Main inputs	Key outputs	Time scale / update rate
Physical simulation layer	Current and planned controls $U(t)$, parameter ensemble X, wellbore / reservoir configuration	Predicted pressure and flow trajectories, influx volumes, fracture margin indicators	Seconds to minutes, depending on model fidelity and ensemble size
Probabilistic inference layer	Simulation outputs, prior parameter distributions, measurement residuals	Updated parameter distributions $f_X(x\|D(t))$, revised risk metrics $P_{\text{kick}}(t)$, $R(T)$	At measurement update times; typically minutes to tens of minutes
Data-driven detection layer	Raw and preprocessed sensor streams, feature vectors x_k	$\hat{P}_{\text{ML}}(t)$, anomaly scores, classification labels with confidence measures	Near real time (seconds) for streaming monitoring
Decision support layer	Combined risk indicators, operational constraints, candidate actions $\mathcal{U}$	Recommended control actions, alert levels, what-if comparisons across options	Event-driven; triggered when risk indices cross predefined thresholds
Monitoring and visualization layer	Historical and real-time risk indices, model diagnostics, operational context	Dashboards, trend plots, audit trail of risk estimates and decisions	Continuous during operations and for post-well review

noise, a typical observation model may be written as

$$Z = h\left(Y(\cdot; x)\right) + \eta, \tag{4.7}$$

where h maps model outputs to the measured quantities, possibly including downsampling and aggregation. Assuming Gaussian noise with covariance Σ_η, the log-likelihood can be expressed as a quadratic form in the residuals between measured and modeled signals [40].

In real-time applications, updating the full posterior distribution may be computationally demanding. Sequential Monte Carlo methods and ensemble-based techniques offer approximate alternatives. In an ensemble Kalman framework, an ensemble of parameter realizations $\{X^{(k)}\}$ is propagated through the deterministic model, and ensemble statistics are updated when new measurements arrive. The analysis update for each ensemble member can be written as [41]

$$X_{\text{a}}^{(k)} = X_{\text{f}}^{(k)} + K\left(Z + \epsilon^{(k)} - h\left(Y_{\text{f}}^{(k)}\right)\right), \tag{4.8}$$

where subscripts f and a denote forecast and analysis, K is a gain matrix computed from ensemble covariances, and $\epsilon^{(k)}$ are perturbed observations consistent with measurement noise. The updated ensemble approximates the posterior distribution and can be used to recompute risk indices $R(T)$ and probabilities $P_{\text{kick}}(t)$.

Table 8: Illustrative control actions and their qualitative impact on kick-related risk

Control action	Expected impact on bottom-hole pressure and influx	Risk trade-offs and considerations
Increase mud density	Raises hydrostatic pressure, reducing likelihood of underbalanced conditions and further influx	May approach or exceed fracture pressure; increases circulating pressures and equivalent circulating density
Reduce pump rate	Lowers frictional pressure losses and can reduce transient underbalance during operations	May delay transport of gas to surface and reduce strength of detection signals in flow-out
Increase annular back-pressure (MPD)	Directly elevates bottom-hole pressure while maintaining circulation	Requires reliable control and equipment; overcompensation can elevate loss risk
Shut in the well	Stops further influx if implemented promptly; stabilizes boundary conditions for well control procedures	Rapid shut-in can generate pressure transients; timing must consider current influx volume and margins
Circulate out influx with controlled choke schedule	Gradually removes gas while managing pressures within pore–fracture envelope	Requires accurate model-based design and monitoring; sensitive to parameter and measurement uncertainty

Validation of probabilistic risk metrics is an important step. Because kick events are relatively rare, direct empirical estimation of probabilities from event frequencies is limited [42]. Instead, assessment relies on internal consistency checks, comparison with historical data, and stress tests under synthetic scenarios. One approach is to generate synthetic kicks using the deterministic model under sampled parameter sets and to compare the distribution of simulated detection times, influx volumes, and pressures with available operational records. Statistical goodness-of-fit measures can be used to evaluate the match between simulated and observed distributions, recognizing the limitations of sparse data [43].

In addition to event probabilities, diagnostic metrics can be defined to support decision-making. For example, the probability that bottom-hole pressure remains between pore and fracture pressures over a future time window $[t, t+\tau]$ can be expressed as

$$P_{\text{safe}}(t,\tau) = \mathbb{P}\left(p_p(z_{\text{bh}};X) + \Delta p_{\min} \le p_{\text{bh}}(s;X) \le p_{\text{frac}}(z_{\text{bh}};X) - \Delta p_{\text{frac}},\ \forall s \in [t,t+\tau]\right), \tag{4.9}$$

where p_{frac} is fracture pressure and Δp_{frac} is a margin. Estimation of such path-dependent probabilities typically relies on approximations, such as discretization of time and evaluation over sampled trajectories, but the resulting quantities provide a more complete description of risk than instantaneous probabilities alone [44].

5. Machine-learning-based detection and early warning

While mechanistic models provide a physically interpretable description of gas kicks, real-time detection often benefits from data-driven methods that can capture complex patterns in noisy signals. Machine-learning approaches can be used to map multi-sensor time series to probabilistic indicators of kick onset, severity, or likelihood of escalation. Such methods can operate in parallel with mechanistic models, using many of the same measurements but without explicit reliance on a particular physical model structure [45].

Consider a set of measured signals $s_j(t)$, $j = 1, \ldots, J$, including flow-out, pump strokes, standpipe pressure, pit volume, choke pressure, downhole pressure, and possibly derived quantities such as rate-of-change or filtered versions. At a given time t_k, these signals and their recent history over a time window $[t_k - \Delta T, t_k]$ are encoded into a feature vector $x_k \in \mathbb{R}^d$. Labels y_k are defined to represent states of interest, for example $y_k = 1$ if a kick is present or likely and $y_k = 0$ otherwise, based on historical annotations or expert interpretation. A supervised learning model seeks a function $f_\theta : \mathbb{R}^d \to [0, 1]$ that estimates the probability of a kick given features, where θ denotes model parameters.

A baseline approach is logistic regression, in which [46]

$$p_\theta(y = 1|x) = \sigma\left(w^\top x + b\right), \tag{5.1}$$

where $\sigma(u) = 1/(1 + e^{-u})$, $w \in \mathbb{R}^d$, and b is a bias term. Parameters are estimated by minimizing the empirical negative log-likelihood

$$J(w, b) = -\frac{1}{N}\sum_{k=1}^{N}\left[y_k \log p_\theta(y_k|x_k) + (1 - y_k)\log\left(1 - p_\theta(y_k|x_k)\right)\right], \tag{5.2}$$

possibly with regularization terms to control model complexity. Although linear in the features, logistic regression can capture non-linear effects if the feature vector includes non-linear transformations of raw signals and their interactions [47].

To more fully exploit temporal structure in the data, recurrent or convolutional neural network architectures can be used. In a recurrent formulation, a hidden state vector h_k evolves as

$$h_k = \phi\left(W_h h_{k-1} + W_x x_k + b_h\right), \tag{5.3}$$

where W_h and W_x are weight matrices, b_h is a bias, and ϕ is a non-linear activation function [48]. The kick probability is then computed as

$$p_\theta(y_k = 1|x_{1:k}) = \sigma\left(v^\top h_k + b_y\right), \tag{5.4}$$

with parameters $\theta = \{W_h, W_x, b_h, v, b_y\}$ learned from data. More advanced variants such as gated recurrent units or long short-term memory cells can improve the handling of long-range temporal dependencies, which are often present in slowly evolving drilling operations.

Training data for kick detection models are typically imbalanced, with many more non-kick than kick samples [49]. This imbalance can be addressed through re-weighting of the loss function, resampling strategies, or specialized metrics for model selection. For example, a weighted loss function can assign higher weight to kick samples, [50]

$$J_\alpha(\theta) = -\frac{1}{N}\sum_{k=1}^{N}\left[\alpha y_k \log p_\theta(y_k|x_k) + (1 - \alpha)(1 - y_k)\log\left(1 - p_\theta(y_k|x_k)\right)\right], \tag{5.5}$$

where $\alpha \in (0, 1)$ is chosen to balance sensitivity and specificity. Performance is evaluated using metrics such as true positive rate, false positive rate, precision, and area under the receiver operating characteristic curve, with particular attention to the trade-off between early detection and false alarms.

Integration with mechanistic models can proceed in several ways [51]. One approach is to use mechanistic simulations to augment training data, especially for rare or extreme scenarios that are poorly represented in historical records. Synthetic signals generated by the deterministic model under varied conditions and parameter realizations can be fed into the same feature extraction and learning pipeline, labeled according to modeled kick states. This helps the machine-learning model generalize to situations that have not yet occurred operationally but are physically plausible [52]. Another approach is to incorporate mechanistic quantities as features, for example predicted bottom-hole pressure or modeled influx

rates under different parameter assumptions, thus combining physics-based predictions with observed signals.

From a mathematical perspective, the machine-learning component provides an approximate mapping from observed data Z to a probabilistic indicator that can be interpreted as an estimate of the conditional probability of a kick,

$$\hat{P}_{\mathrm{ML}}(t_k) = f_\theta(x_k) \approx \mathbb{P}\left(E_{\mathrm{kick}}(t_k)|Z_{1:k}\right). \tag{5.6}$$

This estimate can be treated as one source of information in the probabilistic risk framework, to be combined with outputs from Bayesian updating of mechanistic model parameters [53]. For example, the machine-learning output may be used as a likelihood term or as an additional observation in ensemble-based updating, with an associated noise model reflecting its calibration.

The robustness of machine-learning-based detection depends on the representativeness of training data, the handling of concept drift as drilling practices evolve, and the treatment of missing or corrupted signals. Techniques such as online learning, periodic retraining with new data, and explicit handling of uncertainty in model outputs can mitigate some of these issues [54]. Uncertainty-aware methods, including Bayesian neural networks or ensemble-based prediction intervals, can provide not only point estimates of kick probabilities but also associated confidence measures, which can be valuable for operators making decisions under uncertainty.

6. Integrated risk assessment and mitigation decision framework

The integrated framework combines the deterministic model, probabilistic risk metrics, and machine-learning-based detection into a structure that supports both planning and real-time decision-making. Conceptually, the framework operates as a mapping from available information and operational options to risk metrics and recommended mitigation measures [55]. The mapping is updated as new data arrive and as the drilling state changes.

Let $D(t)$ denote the set of data available up to time t, including raw sensor readings, pre-processed features, and contextual information such as current depth, trajectory, and drilling mode. Let $U(t)$ denote controllable operational inputs, such as pump rate, choke setting, and target mud density [56]. The deterministic model can be written abstractly as

$$Y(t) = \mathcal{M}\left(X, U(\cdot), t\right), \tag{6.1}$$

where X represents uncertain parameters and $\mathcal{M}$ denotes the solution operator of the multiphase flow and reservoir inflow equations. The probabilistic component assigns a distribution to X conditioned on data $D(t)$,

$$f_X(x|D(t)), \tag{6.2}$$

and computes risk metrics such as $P_{\mathrm{kick}}(t)$, $P_{\mathrm{frac}}(t)$, and $R(T)$ as integrals over this distribution. The machine-learning component produces a data-driven indicator $\hat{P}_{\mathrm{ML}}(t)$ using features extracted from $D(t)$. Combining these elements requires a coherent rule for integrating multiple sources of information [57].

One approach is to treat the machine-learning output as an additional observation of an underlying latent variable representing kick likelihood. Let $\Lambda(t)$ denote a latent process summarizing the true but unknown propensity for a kick at time t [58]. The mechanistic-probabilistic model provides a prior distribution for $\Lambda(t)$ given $D(t)$ and $U(t)$, while the machine-learning model yields a noisy observation,

$$\hat{P}_{\mathrm{ML}}(t) = g\left(\Lambda(t)\right) + \epsilon(t), \tag{6.3}$$

where g is a link function and $\epsilon(t)$ represents model error. A Bayesian update can then be performed to synthesize information and yield a posterior distribution for $\Lambda(t)$, from which risk metrics and decision

thresholds can be derived [59]. In practice, this may be approximated through heuristic weighting of model-based and data-driven probabilities, with weights calibrated from historical performance.

Mitigation measures include adjustments in mud density, pump rate, and choke settings, as well as procedural actions such as shutting in the well or initiating circulation to remove gas. These actions can be represented as elements of a control set $\mathcal{U}$. For each candidate control action $u \in \mathcal{U}$, the deterministic model can predict the evolution of pressures and flows over a future time window, subject to uncertainties in X. Risk metrics can then be computed under each control and compared [60]. Formally, for a given action u and time horizon T, define a control-specific risk index

$$R_u(T) = \mathbb{E}\left[C\left(V_{\text{inf}}^u(T; X)\right) \,\middle|\, D(t) \right], \tag{6.4}$$

where V_{inf}^u is the influx volume under control u. The decision problem can be cast as choosing an action that minimizes expected risk subject to operational constraints, such as equipment limits and regulatory requirements.

In practice, several simplifying assumptions are often introduced to render this optimization tractable in real time [61]. One is to parameterize the control space in terms of a small number of discrete options, such as "continue drilling," "reduce pump rate," "increase back-pressure," or "shut in." Another is to use pre-computed response surfaces or surrogate models that approximate $R_u(T)$ as functions of a small set of state variables. These response surfaces can be generated offline using the deterministic model and a range of uncertainty realizations, then queried rapidly during operations.

An example of a composite risk index suitable for real-time use is [62]

$$\mathcal{R}(t) = w_1 P_{\text{kick}}(t) + w_2 P_{\text{frac}}(t) + w_3 \hat{P}_{\text{ML}}(t), \tag{6.5}$$

where w_1, w_2, w_3 are non-negative weights reflecting the relative importance of different risk components and detection layers. Operational thresholds on $\mathcal{R}(t)$ can be defined to trigger alerts or specific mitigation actions. The dependence of $\mathcal{R}(t)$ on uncertain parameters and modeling choices should be examined during planning, so that thresholds are set with an understanding of their sensitivity.

An additional dimension of the framework concerns human factors and organizational procedures. The outputs of the risk assessment need to be communicated in a way that supports operator understanding and decision-making without overloading attention [63]. Quantitative risk indices can be mapped to qualitative categories, such as low, moderate, or elevated risk, with associated recommended actions. The mapping should be calibrated empirically to avoid systematic over- or under-reaction to particular patterns of signals. Logging of risk indicators, decisions, and outcomes supports later analysis and iterative refinement of both models and procedures [64].

From a numerical standpoint, integrating deterministic simulation, probabilistic updating, and machine-learning prediction requires attention to computational loads and latencies. The deterministic simulator may be run at reduced spatial resolution or with simplified physics during real-time operations, while more detailed models are used in planning or off-line analysis. Sampling-based uncertainty propagation can be approximated with small ensembles, possibly combined with linearization techniques [65]. Machine-learning models should be selected not only based on predictive accuracy but also on computational efficiency and robustness to missing or delayed inputs.

The integrated framework is intended to be flexible enough to accommodate different levels of model sophistication and data availability [66]. In wells with limited instrumentation, the machine-learning component may play a smaller role and the probabilistic analysis may rely more heavily on prior distributions and offset-well data. In wells with extensive real-time monitoring, including downhole sensors, more detailed models and richer data-driven components can be deployed. In all cases, maintaining a clear separation between model assumptions, data inputs, and resulting risk metrics helps ensure transparency and facilitates continuous improvement [67].

7. Conclusion

Gas kick events in complex drilling environments involve coupled physical and decision-making processes that span reservoir inflow, multiphase wellbore hydraulics, surface equipment behavior, and human response. This paper has outlined a risk assessment framework that integrates deterministic modeling, probabilistic metrics, and machine-learning-based detection to provide a structured view of these processes. The deterministic component employs one-dimensional conservation laws with appropriate closure relations to describe gas-liquid flow in the wellbore, formation inflow, and surface boundary conditions, with attention to numerical implementation considerations such as stability and computational efficiency [68]. This mechanistic representation enables prediction of key quantities such as bottom-hole pressure evolution, influx volume, and surface detection signals under varied operational scenarios and parameter assumptions.

On top of the deterministic model, a probabilistic layer characterizes uncertainties in formation properties, equipment behavior, and operational conditions through parameter distributions and Bayesian updating. Risk metrics such as probabilities of kick onset, fracture exceedance, and influx severity, as well as composite indices based on expected consequences, are derived as functionals of the induced distributions of model outputs [69]. Sequential updating methods, including ensemble-based approaches, allow incorporation of real-time measurements to refine parameter estimates and risk metrics as the operation proceeds. This probabilistic perspective makes explicit the dependence of risk assessments on uncertain inputs and provides a basis for evaluating the sensitivity of conclusions to assumptions.

The machine-learning component complements mechanistic modeling by learning patterns in multisensor time series that are associated with kick events [70]. By mapping features extracted from flow, pressure, and related signals to probabilistic indicators of kick likelihood, data-driven models can contribute early warning signals and capture complex interactions that may not be fully represented in simplified physical models. Training on historical and synthetic data, with attention to class imbalance and temporal structure, supports calibration of these models for practical use. Integration of machine-learning outputs with probabilistic mechanistic risk measures can proceed through Bayesian or heuristic weighting schemes, yielding combined indicators that leverage both physics-based and empirical information [71].

The combined framework provides a structure for evaluating mitigation measures such as changes in mud density, pump and choke settings, and procedural actions, by predicting their impact on risk metrics under uncertainty. It also highlights the importance of aligning quantitative risk outputs with operational decision processes and human factors, including clear communication of risk levels and associated recommended actions. While the framework does not eliminate uncertainties or guarantee avoidance of gas kicks, it offers a systematic way to organize information, models, and decisions in complex drilling contexts [72].

Future developments may include more detailed coupling of thermal and compositional effects in the deterministic model, enhanced probabilistic representations of geomechanical and human factors, and adaptation of machine-learning components to evolving operational practices through online learning. Continuous evaluation using operational data, including non-event periods and recorded kicks, can support refinement of model structures, parameter distributions, and decision thresholds. In this way, the framework can be iteratively improved as more information becomes available, maintaining relevance across a range of drilling environments and technological configurations [73].

References

[1] N. Bjorndalen, E. Jossy, J. Alvarez, and E. Kuru, ‘‘Reducing formation damage with microbubble based drilling fluid: Understanding the blocking ability,’’ in *Canadian International Petroleum Conference*, PETSOC, 6 2007.

[2] J. Herndon and D. Smith, ‘‘Plugging wells for abandonment: a state-of-the-art study and recommended procedures,’’ 9 1976.

[3] M. Golbabaei-Asl, A. Povitsky, and L. Ring, ‘‘Cfd modeling of fast transient processes in drilling fluid,’’ in *Volume 7A: Fluids Engineering Systems and Technologies*, American Society of Mechanical Engineers, 11 2015.

[4] C. K. Knutson and C. R. Boardman, ''Assessment of non-destructive testing of well casing,, cement and cement bond in high temperature wells,'' 1 1979.

[5] C.-H. Yang, P.-P. Lu, Y.-M. Cao, M. Xu, Z.-Y. Yu, and P.-F. Cheng, ''Study on the plugging limit and combination of co2 displacement flow control system based on nuclear magnetic resonance (nmr),'' *Processes*, vol. 10, pp. 1342–1342, 7 2022.

[6] F. O. Garzon, J. R. Amorocho, M. Al-Harbi, N. S. Al-Shammari, A. Al-Ruwaished, M. Ayub, W. Kharrat, V. Bugrov, J. R. G. Jacobsen, G. A. Brown, and J. V. Noya, ''Stimulating khuff gas wells with smart fluid placement,'' in *SPE Deep Gas Conference and Exhibition*, SPE, 1 2010.

[7] K. Manikonda, A. R. Hasan, A. Barooah, N. H. Rahmani, M. El-Naas, A. K. Sleiti, and M. A. Rahman, ''A mechanistic gas kick model to simulate gas in a riser with water and synthetic-based drilling fluid,'' in *Abu Dhabi International Petroleum Exhibition and Conference*, p. D012S116R009, SPE, 2020.

[8] P. Ekins, R. Vanner, and J. Firebrace, ''Decommissioning of offshore oil and gas facilities: a comparative assessment of different scenarios.,'' *Journal of environmental management*, vol. 79, pp. 420–438, 12 2005.

[9] P. J. L. Webster, B. Y. C. Leung, J. X. Z. Yu, M. D. Anderson, T. Hoult, and J. M. Fraser, ''Coaxial real-time metrology and gas assisted laser micromachining: process development, stochastic behavior, and feedback control,'' in *SPIE Proceedings*, vol. 7590, pp. 759003–, SPIE, 2 2010.

[10] J. D. Muresan and M. V. Ivan, ''Controversies regarding costs, uncertainties and benefits specific to shale gas development,'' *Sustainability*, vol. 7, pp. 2473–2489, 3 2015.

[11] R. Hicks, W. McDonald, and E. Staffel, ''A prefabricated and automated offshore gas production and dehydration facility,'' in *Offshore Technology Conference*, OTC, 4 1971.

[12] R. Rechard, ''Historical background on assessment the performance of the waste isolation pilot plant,'' 6 1999.

[13] R. Mann, ''Slant hole completion test. final report,'' 7 1993.

[14] M. C. Halim, H. Hamidi, and A. R. Akisanya, ''Minimizing formation damage in drilling operations: A critical point for optimizing productivity in sandstone reservoirs intercalated with clay,'' *Energies*, vol. 15, pp. 162–162, 12 2021.

[15] D. Glowka, ''Recommendations of the workshop on advanced geothermal drilling systems,'' 12 1997.

[16] Z. Wan, J. Luo, X. Yang, W. Zhang, J. Liang, L. Zuo, and Y. Sun, ''The thermal effect of submarine mud volcano fluid and its influence on the occurrence of gas hydrates,'' *Journal of Marine Science and Engineering*, vol. 10, pp. 832–832, 6 2022.

[17] M. A. Islam, A. S. M. Woobaidullah, and B. Imam, ''Streamline simulation study on recovery of oil by water flooding: A real case study on haripur field,'' *Bangladesh Journal of Scientific Research*, vol. 28, pp. 61–72, 1 2016.

[18] R. Guzowski and G. Newman, ''Preliminary identification of potentially disruptive scenarios at the greater confinement disposal facility, area 5 of the nevada test site,'' 12 1993.

[19] M. Murphy, ''Advanced oil recovery technologies for improved recovery from slope basin clastic reservoirs, nash draw brushy canyon pool, eddy county, nm,'' 2 1999.

[20] D. Lvova, A. Shagiakhmetov, B. Seregin, and A. Vasiliev, ''Facilities construction engineering for the avaldsnes section of the johan sverdrup field in the north sea,'' *Energies*, vol. 15, pp. 4388–4388, 6 2022.

[21] S. Vij, S. Narasaiah, A. Walia, and G. Singh, ''Multilaterals: An overview and issues involved in adopting this technology,'' in *SPE India Oil and Gas Conference and Exhibition*, SPE, 2 1998.

[22] M. Hohn, D. Patchen, M. Heald, K. Aminian, A. Donaldson, R. Shumaker, and T. Wilson, ''Measuring and predicting reservoir heterogeneity in complex deposystems. the fluvial-deltaic big injun sandstone in west virginia. final report, september 20, 1991–october 31, 1993,'' 5 1994.

[23] F. R. Rodriguez, A. E. Prasetia, A. Mettai, L. Umar, Y. Y. Thiam, and M. S. Murad, ''Hp/ht exploration well in offshore malaysia pushed automated mpd system to maximum utilization, identifying safest drilling operating window,'' *IADC/SPE Drilling Conference and Exhibition*, 3 2014.

[24] R. Zhang and C. Hao, ''Research on the development of hydraulic flushing caverning technology and equipment for gas extraction in soft and low permeability tectonic coal seams in china.,'' *ACS omega*, vol. 7, pp. 21615–21623, 6 2022.

[25] J. T. Finger and B. J. Livesay, ‘‘Alternative wellbore lining methods: Problems and possibilities,’’ 8 2002.

[26] W. C. Chin and X. Zhuang, ‘‘Parent-child, multilateral well and fracture flow interactions,’’ 1 2020.

[27] K. Harpole, E. G. Durrett, S. Snow, J. Bles, C. Robertson, C. Caldwell, D. Harms, R. King, B. Baldwin, D. Wegener, and M. Navarrette, ‘‘Design and implementation of a co2 flood utilizing advanced reservoir characterization and horizontal injection wells in a shallow shelf carbonate approaching waterflood depletion,’’ 9 2002.

[28] T. W. Pfeifle, F. D. Hansen, and D. L. Lord, ‘‘Parameter justification report for drspall.,’’ 10 2003.

[29] M. Horner, ‘‘Development of high-temperature turbine subsystem technology to a technology readiness status, phase ii. quarterly report, january-march 1981,’’ 4 1981.

[30] ‘‘Peer review of the hot dry rock project at fenton hill, new mexico,’’ 12 1998.

[31] F. Huang, H. Li, K. Ji, Q. Ma, and S. Gou, ‘‘A novel system of geothermal enhanced coalbed methane (gth-ecbm) production: (i) heat extraction modelling,’’ *Geomechanics and Geophysics for Geo-Energy and Geo-Resources*, vol. 8, 9 2022.

[32] M. Stanislawek, ‘‘Analysis of alternative well control methods for dual density deepwater drilling,’’ 11 2004.

[33] A. Matei and N. Ianc, ‘‘Classification of underground mining works within the tg. ocna salt mine from the point of view of gas emissions,’’ *MATEC Web of Conferences*, vol. 354, pp. 28–00028, 1 2022.

[34] B. Patel, T. D. Cooper, S. Hughes, and W. C. Billings, ‘‘The application of advanced gas analysis system complements early kick detection and control capabilities of mpd with added hse value,’’ in *SPE/IADC Managed Pressure Drilling and Underbalanced Operations Conference and Exhibition*, SPE, 3 2012.

[35] J. Sullivan, C. Clark, L. Yuan, J. Han, and M. Wang, ‘‘Life-cycle analysis results for geothermal systems in comparison to other power systems: Part ii.,’’ 11 2011.

[36] A. Manzella, ‘‘Geothermal energy,’’ *EPJ Web of Conferences*, vol. 98, pp. 4004–04004, 8 2015.

[37] K. Manikonda, A. R. Hasan, O. Kaldirim, J. J. Schubert, and M. A. Rahman, ‘‘Understanding gas kick behavior in water and oil-based drilling fluids,’’ in *SPE Kuwait oil and gas show and conference*, p. D043S023R001, SPE, 2019.

[38] J. Sawicki and T. Paczkowski, ‘‘Effect of the hydrodynamic conditions of electrolyte flow on critical states in electrochemical machining,’’ *EPJ Web of Conferences*, vol. 92, pp. 02078–, 5 2015.

[39] C. Yang, J. Jiang, B. Qi, G. Cui, L. Zhang, Y. Chen, and P. Cao, ‘‘Experimental and numerical analysis of flow behavior for reverse circulation drill bit with inserted swirl vanes,’’ *Geofluids*, vol. 2022, pp. 1–13, 1 2022.

[40] ‘‘Contaminant plumes containment and remediation focus area. technology summary,’’ 6 1995.

[41] G. Buslaev, P. Tsvetkov, A. Lavrik, A. Kunshin, E. Loseva, and D. Sidorov, ‘‘Ensuring the sustainability of arctic industrial facilities under conditions of global climate change,’’ *Resources*, vol. 10, pp. 128–128, 12 2021.

[42] Y. Redutskiy, ‘‘Oilfield development and operations planning under geophysical uncertainty,’’ *Engineering Management in Production and Services*, vol. 9, pp. 10–27, 9 2017.

[43] J. L. Morrison, ‘‘Establishment of an industry-driven consortium focused on improving the production performance of domestic stripper wells,’’ 9 2001.

[44] V. Simlote and C. Hearn, ‘‘Paddle river gas field, alberta, canada - evaluation of gas reserves and future operating strategy,’’ in *SPE Annual Fall Technical Conference and Exhibition*, SPE, 10 1978.

[45] G. R. Darmawan, N. B. Sangka, S. D. Susilo, J. T. Shaun, S. W. Nas, A. E. Prasetia, and S. Sisworo, ‘‘Integrated downhole isolation valve and managed pressure drilling to facilitate development of sour fractured-limestone gas reservoir in east java, indonesia,’’ *SPE/IADC Drilling Conference and Exhibition*, 3 2011.

[46] T. Huszar, G. Wittenberger, and E. Skvarekova, ‘‘Warning signs of high-pressure formations of abnormal contour pressures when drilling for oil and natural gas,’’ *Processes*, vol. 10, pp. 1106–1106, 6 2022.

[47] ‘‘Research of the lost circulation curing,’’ *Acta Montanistica Slovaca*, pp. 582–592, 12 2021.

[48] ‘‘The objectives for deep scientific drilling in yellowstone national park,’’ 1 1987.

[49] J. L. Smalley, ''A safety equipment list for rotary mode core sampling systems operation in single shell flammable gas tanks,'' 5 1999.

[50] Y. Cheng, L. Wang, H. Liu, S. Kong, Q. Yang, J. Zhu, and Q. Tu, ''Definition, theory, methods, and applications of the safe and efficient simultaneous extraction of coal and gas,'' *International Journal of Coal Science & Technology*, vol. 2, pp. 52–65, 5 2015.

[51] ''Characterize and explore potential sites and prepare research and development plan (site investigation study). final draft. task 2. milestone report,'' 12 1980.

[52] C. Stone, ''Geothermal energy abstract sets. special report no. 14,'' 1 1985.

[53] R. C. Thompson, B. Murphy, K. Williams, H. S. Giberson, J. Garaghty, and G. Pace, ''Energy storage for natural gas fueled electric drilling rigs,'' *SPE/IADC Drilling Conference*, 3 2013.

[54] O. T. Gudmestad and K. Traa, ''Sustainable use and production of energy in the 21st century,'' *International Journal of Energy Production and Management*, vol. 1, pp. 1–15, 6 2015.

[55] G. T. Program, ''Federal geothermal research program update fiscal year 2003,'' 3 2004.

[56] F. Zhang, S. Z. Miska, M. Yu, E. Ozbayoglu, and N. Takach, ''An eulerian approach for characterization of solid suspension in multiphase flow systems and its application in hole cleaning during drilling,'' in *Volume 7: Fluids Engineering*, American Society of Mechanical Engineers, 11 2016.

[57] V. Volovetskyi, Y. Doroshenko, S. Stetsiuk, S. Matkivskyi, O. Shchyrba, Y. Femiak, and G. Kogut, ''Development of foam-breaking measures after removing liquid contamination from wells and flowlines by using surface-active substances,'' *Journal of Achievements in Materials and Manufacturing Engineering*, vol. 114, pp. 67–80, 10 2022.

[58] B. Guo and A. Ghalambor, ''An innovation in designing underbalanced drilling flow rates: A gas-liquid rate window (glrw) approach,'' in *IADC/SPE Asia Pacific Drilling Technology*, SPE, 9 2002.

[59] M. Zoback, ''Scientific drilling into the san andreas fault and site characterization research: Planning and coordination efforts. final technical report,'' 8 1998.

[60] M. Reich, M. Oesterberg, H. Montes, and J. Treviranus, ''Straight down to success: Performance review of a vertical drilling system,'' in *SPE Annual Technical Conference and Exhibition*, SPE, 10 2003.

[61] J. C. Helton, D. Anderson, and B. Baker, ''Computational implementation of a systems prioritization methodology for the waste isolation pilot plant: A preliminary example,'' 4 1996.

[62] R. G. R. Giridhar, P. S. P. Satyanarayana, and T. N. D. T. Nancharaiah, ''Reduction of drilling machine problems during the operation of blast furnace in steel plant,'' *Indian Journal of Applied Research*, vol. 3, pp. 183–185, 10 2011.

[63] A. Sircar, K. Solanki, N. Bist, and K. Yadav, ''Enhanced geothermal systems – promises and challenges,'' *International Journal of Renewable Energy Development*, vol. 11, pp. 333–346, 12 2021.

[64] J. S. S. Toralde and C. Wuest, ''Riser gas risk mitigation with advanced flow detection and managed pressure drilling technologies in deepwater operations,'' in *Offshore Technology Conference-Asia*, OTC, 3 2014.

[65] K. Craik, G. Ju, J. Peterson, B. James, and K. PCastleman, ''Development and implementation of a top-tensioned riser for drilling, completion and producing operations,'' in *Offshore Technology Conference*, OTC, 5 2002.

[66] R. Maglione and G. Robotti, ''Field rheological parameters improve stand pipe pressure prediction while drilling,'' in *SPE Latin America/Caribbean Petroleum Engineering Conference*, SPE, 4 1996.

[67] V. A. Schmidt, B. Crager, and G. Rodenbusch, *Encyclopedia of Maritime and Offshore Engineering - Historical Development of the Offshore Industry*. Wiley, 4 2017.

[68] K. Witwer, ''Test plan for core drilling ignitability testing,'' 1 1996.

[69] C. Carson, ''Suggested drilling research tasks for the federal government,'' 4 1984.

[70] K. Manikonda, A. R. Hasan, O. Kaldirim, N. Rahmani, and M. A. Rahman, ''Estimating swelling in oil-based mud due to gas kick dissolution,'' in *International conference on offshore mechanics and arctic engineering*, vol. 84430, p. V011T11A039, American Society of Mechanical Engineers, 2020.

[71] S. O. Osisanya, A. T. Ayokunle, B. Ghosh, and A. Suboyin, ‘‘Modified horizontal well productivity model for a tight gas reservoir subjected to non-uniform damage and turbulence,’’ *Energies*, vol. 14, pp. 8334–8334, 12 2021.

[72] S. Neacşu and R. Rădulescu, ‘‘Increasing calculation accuracy in the design stage of a gas transportation system,’’ *Analele Universitatii ”Ovidius” Constanta - Seria Chimie*, vol. 24, pp. 61–66, 12 2013.

[73] ‘‘Contracts for field projects and supporting research on enhanced oil recovery. progress review no. 82, quarterly report, january–march 1995,’’ 6 1996.